New Phytologist

Research

Decades-old carbon reserves are widespread among tree species, constrained only by sapwood longevity

Drew M. P. Peltier[1], **Mariah S. Carbone**[2,3], **Kiona Ogle**[2,3,4], **George W. Koch**[2,3] and **Andrew D. Richardson**[3,4]

[1]School of Life Sciences, University of Nevada, Las Vegas, Las Vegas, NV 89154, USA; [2]Department of Biological Sciences, Northern Arizona University, Flagstaff, AZ 86011, USA; [3]Center for Ecosystem Science and Society, Northern Arizona University, Flagstaff, AZ 86011, USA; [4]School of Informatics, Computing, and Cyber Systems, Northern Arizona University, Flagstaff, AZ 86011, USA

Author for correspondence:
Drew M. P. Peltier
Email: drew.peltier@unlv.edu

Received: *12 July 2024*
Accepted: *13 November 2024*

New Phytologist (2024)
doi: 10.1111/nph.20310

Key words: bomb spike, carbon allocation, carbon starvation, NSC, radiocarbon, sink limitation, storage.

Summary

- Carbon reserves are distributed throughout plant cells allowing past photosynthesis to fuel current metabolism. In trees, comparing the radiocarbon ($\Delta^{14}C$) of reserves to the atmospheric bomb spike can trace reserve ages.
- We synthesized $\Delta^{14}C$ observations of stem reserves in nine tree species, fitting a new process model of reserve building. We asked how the distribution, mixing, and turnover of reserves vary across trees and species. We also explored how stress (drought and aridity) and disturbance (fire and bark beetles) perturb reserves.
- Given sufficient sapwood, young (< 1 yr) and old (20–60+ yr) reserves were simultaneously present in single trees, including 'prebomb' reserves in two conifers. The process model suggested that most reserves are deeply mixed (30.2 ± 21.7 rings) and then respired (2.7 ± 3.5-yr turnover time). Disturbance strongly increased $\Delta^{14}C$ mean ages of reserves (+15–35 yr), while drought and aridity effects on mixing and turnover were species-dependent. Fire recovery in *Sequoia sempervirens* also appears to involve previously unobserved outward mixing of old reserves.
- Deep mixing and rapid turnover indicate most photosynthate is rapidly metabolized. Yet ecological variation in reserve ages is enormous, perhaps driven by stress and disturbance. Across species, maximum reserve ages appear primarily constrained by sapwood longevity, and thus old reserves are probably widespread.

Introduction

The sizes, distributions, and cycling of pools of nonstructural carbohydrates (NSCs) – or carbon reserves – represent central quantities of fundamental importance in understanding the ecology and physiology of trees (Chapin *et al.*, 1990; Dietze *et al.*, 2014). Trees are long-lived, immobile organisms, and thus experience widely varied conditions throughout their lifespans (Piovesan & Biondi, 2021). Tolerating extreme events such as disturbances while taking advantage of favorable conditions is thus essential. The storage of carbon reserves represents one strategy contributing to such resilience, where photosynthate can be saved for periods of metabolism that are unfavorable to photosynthesis, including poor seasons (Furze *et al.*, 2020), years (Adams *et al.*, 2013), or decades (Kobe, 1997). Reserves thus play a key role in supporting tree resilience to a variety of disturbances such as hurricanes, drought, fire, frost, and insect attack (Vargas *et al.*, 2009; Hagedorn *et al.*, 2016; Wiley *et al.*, 2016; D'Andrea *et al.*, 2019; Reed & Hood, 2023). Moreover, as reserves become remobilized to support respiration, severe exhaustion may be catastrophic, where reserve pool size is implicated as a critical indicator of mortality risk from drought (Dickman *et al.*, 2015; McDowell *et al.*, 2022), among other stressors. Reserve pools are also regularly leveraged for seasonal leaf production (Schädel *et al.*, 2009), reproduction (Ichie *et al.*, 2013; Hesse *et al.*, 2021; Kabeya *et al.*, 2021), defense (Huang *et al.*, 2019), and growth (Barbaroux & Bréda, 2002; Muhr *et al.*, 2016).

The dynamics of reserve cycling over long time periods remains poorly understood (Hartmann & Trumbore, 2016). If relying solely on concentration (pool size) measurements, clever design of experiments and exhaustive, repeated sampling across organs is necessary to capture the rapid dynamics in reserve pools (Hagedorn *et al.*, 2016), or dynamics that do not result in changes in total concentrations. This may be one explanation for inconsistent findings regarding, for example, the responses of reserves to drought. Different studies find reserve concentrations decrease, are maintained, or even increase in certain organs during drought conditions (Anderegg & Anderegg, 2013; Palacio *et al.*, 2014; Dickman *et al.*, 2015). So-called 'pulse-chase' labelling approaches have often been used to study the fluxes of reserves through trees, for example from leaves to sinks like wood and roots (Kagawa *et al.*, 2006; Epron *et al.*, 2012). However,

New Phytologist

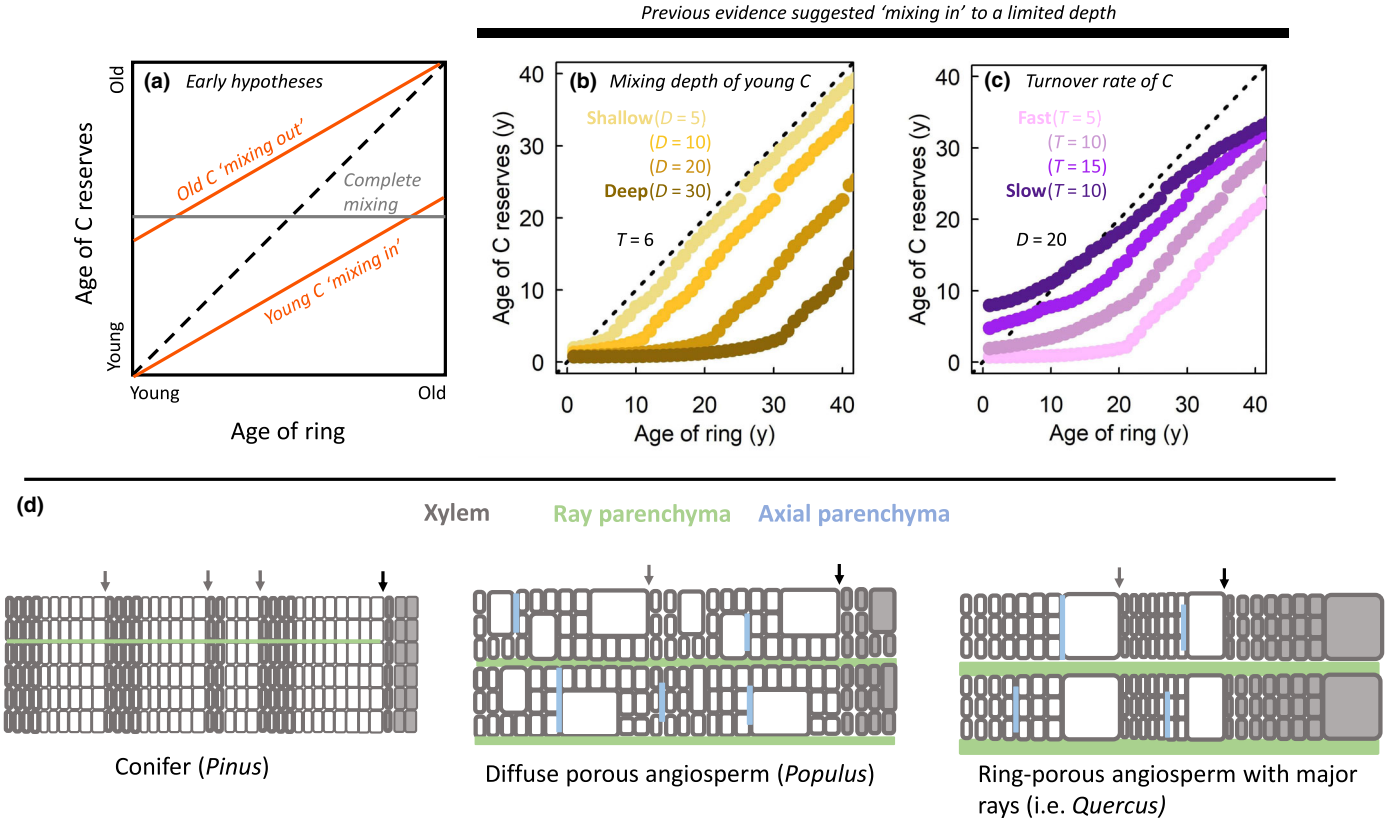

Fig. 1 Illustration of theory and anatomy of the distribution of carbon reserves in tree sapwood. (a) Early hypotheses (Richardson *et al*., 2015) investigated whether old reserves were 'mixed out' and into younger rings (above dashed 1 : 1 line) or young reserves were 'mixed in' to older rings (below dashed 1 : 1 line). (b, c) Evidence is consistent with 'mixing in' to a limited depth. Our process model incorporates (b) mixing depth, where deeper mixing (darker yellow lines) moves the inflection point deeper into older rings, and (c) turnover time of reserves (driven by respiration), where slower turnover (darker purple lines) produces reserve ages close to ring age. (d) Carbon reserves are stored in parenchyma cells in the phloem (dark green), rays (medium green), and axially among sapwood (light green, more common in angiosperms). Simplified distribution of xylem and parenchyma are shown in coniferous wood (left), diffuse-porous angiosperm wood (center), and ring-porous angiosperm wood (right). The symbol '. . ..' denotes an omitted section of sapwood rings; heartwood is shaded gray. In (b, c), points are ring-wise predictions generated from the process model where parameter values of mixing depth (*D*) and turnover time (*T*) are reported for each simulation.

because the 'pulse' is often short-lived (Furze *et al*., 2019a; Rehschuh *et al*., 2022), these labelling approaches are less useful to study the dynamics of reserves at multidecadal timescales. Adding to this challenge, most reserve measurements focus on organs with short lifespans (leaves, twigs, and small roots) that may bias estimates of the cycling rates of total tree carbon reserves.

The largest pool of carbon reserves in trees resides in the bole and coarse woody tissues (Hoch *et al*., 2003), and the dynamics of this pool are highly uncertain. While large, the utility of this deeply stored reserve carbon has sometimes been unclear. For example, seasonal patterns of refilling and moderate drawdown associated with deciduous leaf phenology have been observed (Barbaroux & Bréda, 2002; Furze *et al*., 2019b). At the same time, observations of strong exhaustion of this reserve pool in large, mature trees are uncommon (Peltier *et al*., 2023b). This may suggest that not all stem carbon reserves are 'available' (Sala *et al*., 2012), or perhaps these reserves are simply too far from the sites of high metabolic carbon demand (Schädel *et al*., 2009; Anderegg & Callaway, 2012; Blumstein *et al*., 2024). However, another interpretation is that bole carbon reserves represent a large emergency reserve built up over many years, where radiocarbon studies suggest that very old carbon pools can be accessed following severe disturbance (Vargas *et al*., 2009; Carbone *et al*., 2013; Muhr *et al*., 2018; Peltier *et al*., 2023a).

Radiocarbon ($\Delta^{14}C$) dating of carbon reserves could be a powerful tool to understand the long-term storage of energy in trees (Fig. 1). By quantifying the amount of ^{14}C in a pool of reserves, the ^{14}C mean age (or time-since-fixation) can be estimated by reference to the atmospheric record of bomb-derived ^{14}C (Levin & Kromer, 2004; Hua *et al*., 2022). This allows for direct inference on the turnover time (Herrera-Ramírez *et al*., 2020) of large (Hoch *et al*., 2003) and decades-old (Carbone *et al*., 2013) pools of reserve carbon in trees. This approach demonstrated the oldest reserves are typically found in old sapwood rings, where the age of reserves is younger than the associated structural tissue (Richardson *et al*., 2015). This 'mixing in' of current photosynthate into reserve pools suggests that trees continue to invest new carbon into sapwood storage over many years (Fig. 1a). But radiocarbon methods remain underutilized, and our understanding of the dynamics of large and persistent bole pools of carbon reserves remains nascent.

Past research has focused on mean and maximum ages, but existing data represent a deep well of information with which to investigate ecological variation in reserve ages, and could be used to inform new process models. Simplified process representations of carbon allocation dynamics can also be used to learn about carbon reserve cycling (e.g. Oswald & Aubrey, 2023). Two key processes by which bole reserve pools change over time include: 'mixing' of new photosynthate into extant sapwood (Fig. 1b); and 'turnover' (loss) of reserves to respiration or export (Fig. 1c). Deeper mixing would move new photosynthate into deeper rings, reducing reserve ages in those rings (Fig. 1b); slower turnover (e.g. via reduced respiration rates) would result in persistence of reserves, thus increasing ages (Fig. 1c). Then, reserve mixing depth and turnover should be responsive to ecological variation in carbon allocation among species and individuals. For example, varied mixing depth across different species could reflect different allocation strategies or wood anatomies (Fig. 1d; Morris *et al.*, 2015), where some species may prioritize allocation to storage (Hartmann & Trumbore, 2016; Huang *et al.*, 2021). Angiosperms (vs conifers) typically have more sapwood parenchyma (Fig. 1d) and larger stem reserve pools, but may have more rapid turnover if deciduous (Furze *et al.*, 2019b). The distribution of old carbon reserves might also reflect adaptations to catastrophic disturbance, which can remobilize very old reserves (Vargas *et al.*, 2009; Carbone *et al.*, 2013; Muhr *et al.*, 2018; Peltier *et al.*, 2023a).

In this study, we ask: (Q1) how deeply do trees of different species mix new carbon reserves into sapwood (i.e. how many sapwood rings)?; (Q2) how quickly are stored carbon reserves lost from sapwood in different tree species?; and, (Q3) how do stress (e.g. drought and aridity) and disturbance (fire and beetles) perturb reserve ages, mixing depth, and turnover? We addressed these questions by synthesizing published and newly collected $\Delta^{14}C$ data of observations of sapwood carbon reserve ages (Fig. 2) for deciduous angiosperms (including oaks) and conifers, including trees experiencing stress and/or disturbance (drought, fire, bark beetles). With these data, we developed a new process model to simulate the distribution of carbon reserves across sapwood rings. Our overarching goal was to improve our understanding of the ecological drivers of variation in $\Delta^{14}C$ mean age of reserves stored in, and used by, trees.

Materials and Methods

Compilation of existing carbon reserve age data

We compiled sapwood carbon reserve age estimates from five published studies (Richardson *et al.*, 2015; Peltier *et al.*, 2023a,b,c,d) supplemented with new collections (Supporting Information Dataset S1). In all cases, sapwood was primarily identified based on visual assessment of wood color, secondarily aided by moisture content. Explicit (reported) ring numbers are necessary to link carbon reserve age to a ring formation year in our process model (described below). A model expressed instead in terms of depth increments could be a target for future work. The combined dataset thus includes 267 subsamples of stem reserve age and size (concentration) in 52 trees from nine species (*Populus tremuloides* Michx., *Pinus contorta* Dougl. ex Loud., *Pinus edulis* Engelm., *Pinus ponderosa* Dougl. ex Laws., *Pinus strobus* L., *Pseudotsuga menziesii* (Mirb.) Franco, *Sequoia sempervirens* (D. Don) Endl., *Quercus gambelii* Nutt., and *Quercus rubra* L.) at 10 sites (Fig. 2). These subsamples are subsections from stem cores or stem cross-sections, where each subsample contains one to several rings. For five species, reserve ages were also estimated in living bark ($n = 39$ subsamples, hereafter 'phloem').

Richardson *et al.* (2015) described harvesting of two young trees in Harvard Forest (northeastern USA), one eastern white pine (*P. strobus*, 23 yr old), and one northern red oak (*Q. rubra*, 30 yr old). Reserve ages were measured via extractions (Czimczik *et al.*, 2014), and concentrations were measured with an early version of the phenol-sulfuric acid method (Chow & Landhäusser, 2004). Because $\Delta^{14}C$ were independently reported for sugar and starch fractions, we aggregated these into a single weighted average $\Delta^{14}C$ for the carbon reserve pool according to associated reported sugar and starch concentrations.

Four additional studies included here used an incubation method, leveraging cellular respiration, to estimate reserve age and size (Peltier *et al.*, 2023c). First, Peltier *et al.* (2023c) described a direct comparison of these two age-assessment methods (extractions vs incubations) in phloem and sapwood for a single 30-yr-old trembling aspen (*P. tremuloides*) harvested near Flagstaff, Arizona (southwestern USA). We note that this study found extraction methods (Czimczik *et al.*, 2014) to overyield, likely including structural carbon, while incubations underyield, as respiration will never completely consume the entire carbon reserve pool. As incubations only respire reserve carbon that is available for respiration, this is our preferred method, and the majority of our dataset is represented by incubation-derived $\Delta^{14}C$. Second, Peltier *et al.* (2023b) described reserve age measurements in a rainfall manipulation study in New Mexico (southwestern USA) in 10 two-needle piñon (*P. edulis*; Fig. 2a); tree ages exceeded 100 yr, four trees were unmanipulated (control), and six trees were exposed to short- or long-term drought. Third, Peltier *et al.* (2023d) compared carbon reserve ages in 12 *P. tremuloides* trees at two sites: a dry, low-elevation site (northern New Mexico), and a wet, high-elevation site (southern Utah, USA; Fig. 2b). Supplementary measurements from two trees in southern Colorado, USA, are included here. Fourth, Peltier *et al.* (2023a) measured sapwood reserve ages in 18 old-growth coast redwood (*S. sempervirens*; Fig. 2c) trees at Big Basin Redwoods State Park (California, USA) during 2021 and 2022. These redwoods survived a wildfire in August of 2020, and range in height from 45 to 80 m; tree ages are unknown but probably exceed 1000 yr in many trees (80–450 cm diameter at breast height (DBH)). An unburned 93 m tall, 646-yr-old *S. sempervirens* in the Santa Lucia Preserve (Monterey County, California) was also sampled in 2021.

Additional data collection

We supplemented these datasets with new collections of ponderosa pine (*P. ponderosa*), lodgepole pine (*P. contorta*), Gambel oak (*Q. gambelii*), and Douglas-fir (*P. menziesii*). In 2023, three *P. ponderosa* and one *Q. gambelii* were sampled in the Flagstaff

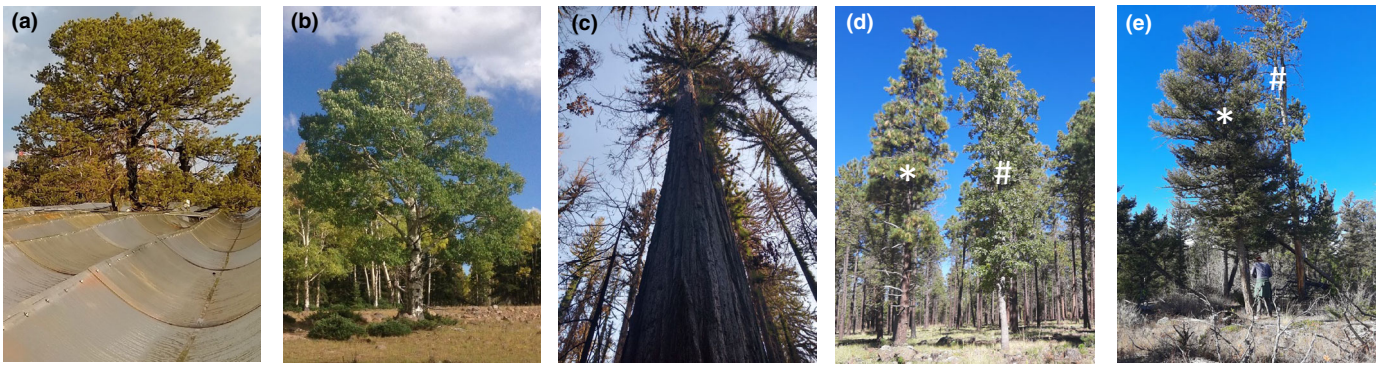

(f)

Species	Family	Leaf habit	Range	Climate	Longevity (yr)	Max ht (m)	*n* (trees)
Pinus contorta	Pinaceae	Evergreen conifer	Western N. America	Mesic	400	45	6 (2)
Pinus edulis	Pinaceae	Evergreen conifer	Southwestern US	Semi-arid	1115	*c*.15	53 (10)
Pinus ponderosa	Pinaceae	Evergreen conifer	Western N. America	Xeric	933		7 (1)
Pinus strobus	Pinaceae	Evergreen conifer	Northeastern US	Mesic	400	55	8 (1)
Populus tremuloides	Salicaceae	Deciduous angiosperm	N. America	Mesic	200	*c*.40	49 (13)
Pseudotsuga menziesii	Pinaceae	Evergreen conifer	Western N. America	Mesic	1300	100*	6 (2)
Quercus rubra	Fabaceae	Deciduous angiosperm	Eastern US	Mesic	400	35	8 (1)
Quercus gambelii	Fabaceae	Deciduous angiosperm	Southwestern US	Mesic	150	35	12 (3)
Sequoia sempervirens	Cupressaceae	Evergreen conifer	Coastal California	Coastal	2500	115.9	75 (19)

Fig. 2 Summary of the assembled $\Delta^{14}C$ dataset. (a–e) Images and (f) descriptions of study species (inset table) including range, climate, maximum longevity, maximum height, and sample size of $\Delta^{14}C$ of trees in parentheses. Maximum longevities and heights are estimates. Images of study species show (a) *Pinus edulis*, (b) *Populus tremuloides*, (c) *Sequoia sempervirens*, (d) *, *Pinus ponderosa* and #, *Quercus gambelii*, (e) *, *Pseudotsuga menziesii* and #, *Pinus contorta*.

area at the Centennial Forest (35.18, −111.76, elevation 2180 m; Fig. 2e); one *P. ponderosa* was infested by bark beetles. Two *P. contorta* and two *P. menziesii* were sampled at the YELL-NEON site in Yellowstone National Park (44.95, −110.53, elevation *c.* 2000 m; Fig. 2f). We estimated reserve ages using the incubation method described in Peltier *et al.* (2023c).

Briefly, 13 mm increment cores (Haglof, Sweden) were collected and sapwood was rapidly subsampled, sectioning sapwood on ring boundaries using a razor blade. Subsamples were placed into sealed 256 ml mason jars where headspace CO_2 was removed with a soda-lime column and pump, and incubated at room temperature. Incubations leverage respiration of reserves in live sapwood. CO_2 is collected after 120 h (5 d) into evacuated air stabilizer cans (LabCommerce, San Jose, CA, USA). The CO_2 is purified on a vacuum line and converted to graphite (Lowe, 1984; Vogel *et al.*, 1984). $\Delta^{14}C$ was measured by accelerator mass spectrometry (AMS) in the Arizona Climate and Ecosystems (ACE) Isotope Laboratory at Northern Arizona University on a Mini-Carbon-Dating System (Synal *et al.*, 2007). $\Delta^{14}C$ are decay- and fractionation-corrected by ACE with standard methods (Stuiver & Polach, 1977; Reimer *et al.*, 2004).

Dating of reserves from $\Delta^{14}C$, and '^{14}C mean ages'

Age estimates from $\Delta^{14}C$ (radiocarbon) measurements are '^{14}C mean ages', but ^{14}C mean ages do not describe the age distribution within a reserve pool. Carbon reserves represent a heterogeneous mixture, as young carbon is continuously added and respired while small amounts of old carbon are retained (Sierra *et al.*, 2017; Muhr *et al.*, 2018). Age of reserves was estimated here by comparing it to the atmospheric bomb spike (Hua *et al.*, 2022), extended by annual plant collections (Peltier *et al.*, 2023a,b,d) and/or extrapolation of the recent trend by 1–3 yr. Lastly, multiple subsamples across sapwood within an individual tree are essential to infer the presence of carbon reserves fixed before the peak of the bomb spike. Here, for samples with $\Delta^{14}C$ values near 0‰, which could be 'prebomb' carbon (60+ yr old) or very recent carbon (*c.* 0 yr old), the location of that subsample within the tree (i.e. radial context) can inform our understanding of the true age of a sample (Trumbore *et al.*, 2015).

Hierarchical statistical model to infer age vs depth trends

We sought to characterize the patterns in reserve ages across sapwood depth (here, equivalent to sapwood age, as ring count), as well as the ecological variability in reserve ages across different tree species and individuals. In our previous work, reserve ages increased with sapwood depth (Fig. 1). Older rings typically contain the oldest reserves (Richardson *et al.*, 2015), though the pattern of increase with depth varies across species. Reserve age in a given ring can also be younger than that ring's age, consistent

with 'mixing in' of newer reserves (Fig. 1a). To quantify the distribution of reserve ages across sapwood rings (and how this differs by species), we fit a hierarchical random-intercepts (tree-level intercepts) regression of carbon reserve age vs sapwood depth (i.e. ring number, where 1 indicates the most recently formed ring). We included quadratic effects of ring age if significant. See supplement for model code.

$$\text{Age}_i \sim a_{\text{tree}} + b_{1,\text{species}} r_i + b_{2,\text{species}} r_i^2 \quad \text{Eqn 1}$$

Because we might expect individuals within a species to vary, but be more similar to each other than to individuals of another species, the model was implemented in a hierarchical Bayesian framework. Thus, for the regression model of reserve age on sapwood depth, tree-level intercepts, a, were given hierarchical priors drawn from species-level intercepts. Species-level effects, b_1 and b_2, were given hierarchical (normal) priors drawn from a single global mean. We report the posterior means and 95% credible intervals of species-level effects. This model was fit using JAGS v.4.0.0 (Plummer, 2003) via the RJAGS package (Plummer, 2013) in R 4.3.1 (R Core Team, 2022); code in Methods S1. The model was run on the high-performance computing cluster at Northern Arizona University ('Monsoon'; https://www.in.nau.edu/arc) with three MCMC chains until convergence, after which we obtained 3000 relatively independent samples of the parameters of interest.

Associated tree-level ecological data

We have measurements of tree height, diameter (DBH), and sapwood depth (as number of tree rings) for most trees in our analysis. To understand possible ecological constraints on maximum reserve ages across species, we used an additional set of (frequentist) linear regressions to explore the potential tree-level drivers of variation in maximum reserve ages across trees. We regressed the oldest measured ^{14}C mean age for each tree on either tree height, DBH, or sapwood depth. For much of the incubation-derived estimates of ^{14}C mean ages, we lack estimates of tree age, so tree age is not included in our analysis.

A process model of sapwood mixing

We constructed a simple process model of radial mixing of reserves into sapwood. See Methods S2 for example code fitting the process model to *P. edulis* data in R. While we report measurements in terms of Δ^{14}C (‰) or ^{14}C mean age of carbon reserves (yr), we parameterize the model in terms of fraction modern ($F^{14}C$; Trumbore *et al.*, 2016), which is independent of sampling date (unlike Δ^{14}C; Trumbore *et al.*, 2016). $F^{14}C$ is a measure of deviation in the $^{14}C:{}^{12}C$ ratio from a standard in 1950 (95% of $^{14}C:{}^{12}C$ of Oxalic Acid I).

The model uses using three key process parameters: mixing depth (D), turnover time of reserves (T), and sapwood depth (D^*). These three process parameters interactively determine the relative size of two pools: a 'fast' pool composed of the proportion of annually fixed carbon that is respired in that same year; and a 'slow' pool built up over time by carbon that is allocated to storage (Richardson *et al.*, 2015; Peltier *et al.*, 2023a). We first describe the sub-model for the slow pool: beginning in 1850, we simulate the annualized addition of reserves to the slow pool (i.e. the storage pool) across years ('compartments') and rings. Compartments track the contributions of unique years' photosynthate to total C in a given ring, for example, the amount of C fixed in 2013 still present in a ring formed in 2023. We thus assume reserves in each ring are well-mixed, and each sapwood ring (up to the sapwood depth D^*) holds a unique mixture of carbon reserves fixed in past years. The amount of ^{14}C added to each compartment in a given ring is driven by the atmospheric $F^{14}C$ record, and the mixing depth (D). In a given year, deeper mixing (larger D) adds more C to deeper sapwood rings, while shallower mixing distributes C across fewer, younger rings. Our model also seeks to simulate that as new carbon is added to the existing reserve carbon (slow pool), some carbon is also lost (reflecting respiration, export, heartwood formation, etc.) according to the turnover time of slow pool C, T_{slow}. We approximate this behavior by only adding the proportion of slow pool carbon not destined to be eventually respired. Then, the slow pool in an individual sapwood ring only becomes completely 'full' just before it transitions to heartwood; more recently formed sapwood rings are comparatively 'empty'. Only after computation of the slow pool do we 'fill up' the remaining space in the total sapwood reserve pool with the current year (collection year) carbon, reflecting the 'fast' pool (more details below).

The 'slow' pool is calculated according to the age distribution of the carbon in stored carbon reserves. We parameterize the slow pool in terms of (unitless) ratios, rather than absolute concentrations of carbohydrates. Thus, for a given tree, the fraction modern of the slow pool, $F^{14}C_r^{\text{slow}}$ for ring r is calculated as a function of two matrices **Q** and **A**, where **Q** describes how new reserve carbon is annually allocated across each ring, r, across Y rings, constrained by D^*. Rings are counted from oldest to youngest, where ring 1 is the oldest (1850) while ring Y is the youngest (e.g. 2023). Thus, **Q** and **A** are of dimension $Y \times Y$, where Y reflects the range of years considered from 1850 up to the year of sampling (2012, 2017, 2020, 2021, or 2023 in this dataset). Within each ring, Y year-specific compartments, c, account for the unique annual contributions of reserve carbon in each of the Y different rings, r. Then, **A** traces the distribution of atmospheric ^{14}C (including the bomb spike) across Y compartments within each of Y rings, reflecting the allocation described in **A**. Each element of these matrices is calculated as follows for each tree:

$$Q_{r,c} = \begin{cases} \left(e^{-\frac{1}{T_{\text{slow}}}}\right)^{r+D-c} & ; c-r < D \\ 0 & ; c-r > D \end{cases} \quad \text{Eqn 2}$$

$$A_{r,c} = \left\{ F^{14}C_c^{\text{atm}} \times Q_{r,c} \right\} \quad \text{Eqn 3}$$

where $F^{14}C^{\text{atm}}$ denotes the atmospheric fraction modern for each compartment, c. D and T_{slow} denote the mixing depth and turnover time of slow pool C. To reflect that new carbon is only mixed D rings deep in a given year, we set $Q_{r,c} = 0$ and $A_{r,c} = 0$

when $c - r$ exceeds D. The ^{14}C-content allocated to storage in a specific ring, $F^{14}C_r^{slow}$, is calculated as the ring-wise ratio of $A_{r,c}$ to $Q_{r,c}$ (a weighted average of $A_{r,c}$), after summing across compartments within each ring:

$$F^{14}C_r^{slow} = \frac{\sum_{c=1}^{Y} A_{r,c}}{\sum_{c=1}^{Y} Q_{r,c}} \quad \text{Eqn 4}$$

where recall Y is the year of the most recent ring, expressed as a number of years after 1849 (e.g. 171 for 2020). This is the fraction modern of the slow pool.

To calculate the fraction modern of all the carbon in a given ring (i.e. to match our actual observations), we 'fill up' the remainder of each ring in the sapwood with current year carbon reserves, according to $F^{14}C^{atm}$ in the sample collection year. Note that this assumes that the turnover of this 'fast' pool of carbon (T_{fast}) is essentially immediate ($T_{fast} \sim 0$ yr), as none is ever added to the slow pool. The predicted fraction modern for a given ring is then an average of that of the fast pool (current year carbon) and that of the slow pool (stored carbon reserves over many past years), weighted by the relative size of these two pools. At this point, we can 'back out' an estimate of the turnover time of the total reserve pool (T) according to the turnover time of the slow pool (T_{slow}), the turnover time of the fast pool ($T_{fast} = 0$), and their relative weights (only the weight for the slow pool is important).

We ignore the radioactive decay of radiocarbon as the half-life is one to two orders of magnitude longer than the period of dynamics being considered here. We fix carbon reserve mass, M_r, for each ring, r, as a proportion (0–1) that linearly declines with sapwood depth, where $M_r = 0$ at depths greater than D^*. This reflects the assumption that reserve masses decrease with sapwood depth, perhaps related to declining surviving parenchyma abundance (Spicer & Holbrook, 2007; Nakaba *et al.*, 2008; Peltier *et al.*, 2023c). As this decline is linear, this also reflects an implicit assumption that reserve masses decline more slowly into deeper rings in trees with more sapwood rings. Alternative parameterizations could be considered in future work.

Finally, these ring-wise $F^{14}C_r$ (fast and slow pool carbon) are aggregated via a weighted average by reserve mass, M_r, to match the subsamples of rings observed in our dataset as:

$$\mu_i = \sum_{r=\text{start}}^{\text{end}} \frac{F^{14}C_r \times M_r}{\sum_{r=\text{start}}^{\text{end}} M_r} \quad \text{Eqn 5}$$

where in the example of a subsample containing the most recently formed (outermost) 10 rings, 'start' would be the deepest ring present in the subsample (the 10th ring) and 'end' would the shallowest (the first ring). In this way, we can compare the ring-wise estimates of $F^{14}C$ to the data-based estimates we produced.

We used this simulation model to identify mean mixing depths and turnover times for each species (Q1 and Q2). However, given that some trees within our dataset may have experienced stress or disturbance such that their carbon reserve pools were not at steady state (Metzler *et al.*, 2018), we also fit the model to different subsets of trees to explore how fire, drought, and aridity influence model parameters (Q3). We explicitly highlight that fitting the steady-state process model to trees not in the steady state could be misleading. Specifically, estimated values of T and D for disturbed trees are not necessarily meaningful as a turnover time or mixing depth, nor are they directly comparable to parameter estimates in healthy trees. However, fitting the model to disturbed trees could be used to assess whether or not disturbance impacts reserve cycling. For example, if parameter estimates for disturbed trees differ substantially from healthy trees, this could inform our understanding of how different disturbances perturb tree carbon reserve cycling.

Thus, for *S. sempervirens*, we fit the same model individually to the unburned tree and compared it to values obtained for burned trees. Similarly, for *P. edulis*, we fit the model individually to trees experiencing short-term drought, long-term (decadal) drought, or control conditions. For *P. tremuloides*, we fit the model individually to a wet site and a chronically dry site. For *P. ponderosa*, we fit the model to a tree that was being attacked by bark beetles and compared it to two healthy trees.

Implementation of sapwood mixing process model

Parameter estimates for the process model were made with genetic algorithms from the GA package in R. This allows for box constraints, for which we specified {1, D^*} for both turnover time and mixing depth. The optimization criterion was negative sum of squares error (SSE), because these algorithms maximize. Because of small sample sizes for certain species we performed jacknife estimation of uncertainty, where for each species we estimated $(n - 1)$ parameters sets with one observation omitted. We report uncertainty as the SD of these replicate estimations. Different algorithms may return different results: we also performed parameter estimations with a variety of algorithms (i.e. simulated annealing) using the 'optim' function in R, but these proved highly sensitive to initial values. Finally, genetic algorithms performed poorly for a single species (*P. ponderosa*) unless we excluded observations that obviously included 'prebomb' carbon (see the Results section). Thus, for this species only, we generated parameter estimates and associated uncertainty using only observations dominated by 'postbomb' carbon. For all species, we used mean parameter estimates to generate age predictions from the process model and evaluated fit to the observed data with R^2 between predicted and observed dated ages of carbon reserves.

Results

Ages differ across individuals and species

Reserve ages increased with sapwood depth in healthy trees, but species exhibit broad ecological variability (Fig. 3). For example, ^{14}C mean ages varied from < 1 to > 36 yr old. In some cases, variation among individuals of a species could be as large as

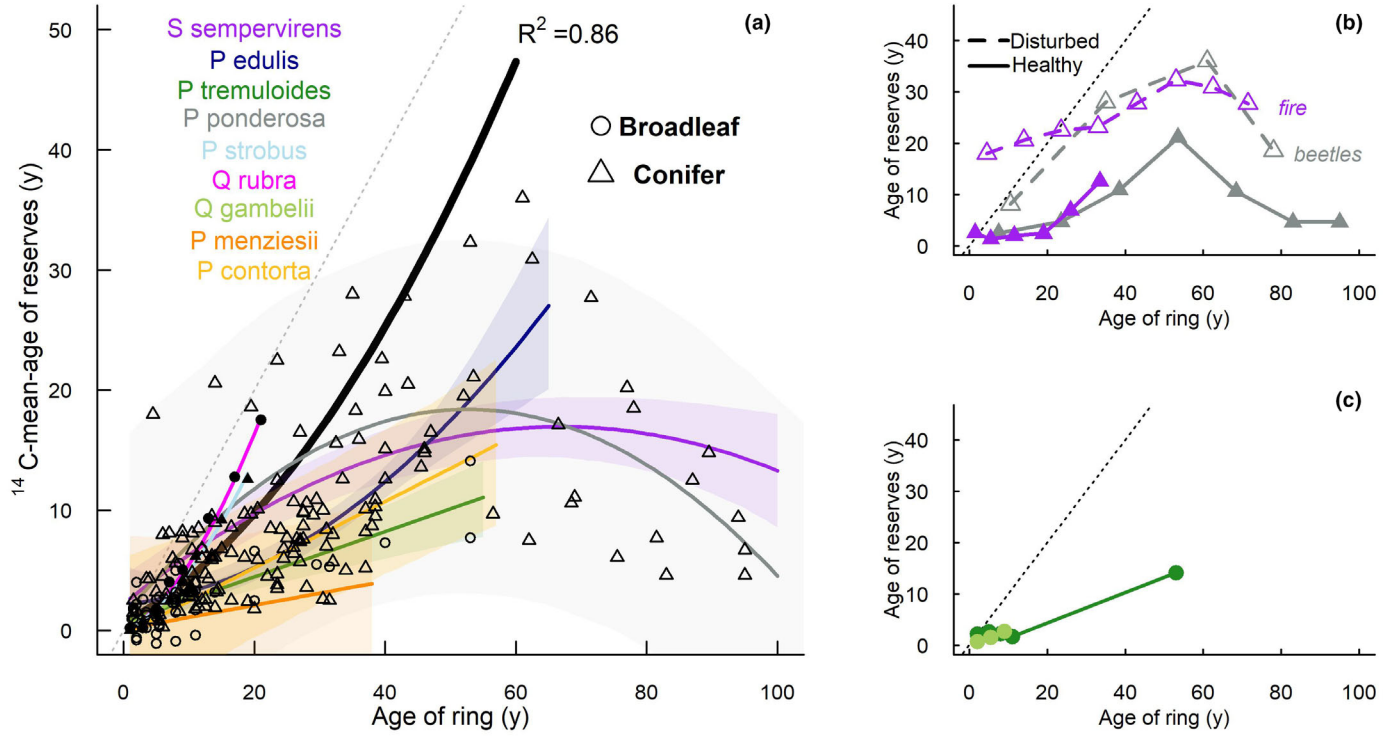

Fig. 3 Combined dataset of carbon reserve ages across the sapwood of all 52 trees of nine species. (a) Dated ages (years) of carbon reserves and lines of best fit (lines and shading) are shown for each of the nine species. Triangles denote conifers, circles denote angiosperms. Unfilled symbols are derived from incubation methods; filled symbols from extraction methods. Thick black line is overall across-species line of best fit ($R^2 = 0.86$). All $\Delta^{14}C$ of sapwood carbon reserves are reported in the supplement. Example individual (b) conifers and (c) angiosperms illustrate the range of variability within a species. (b) A healthy (solid line, filled triangles) and disturbed (dashed line, unfilled triangles) tree of each of *Pinus ponderosa* (gray) and *Sequoia sempervirens* (purple). (c) Healthy *Quercus gambelii* and *Populus tremuloides* trees with differing sapwood depths. In (b, c), samples for each tree extend to the heartwood boundary. Dotted gray line represents the ring (cellulose) age (1 : 1 line). Age uncertainty due to accelerator mass spectrometry (AMS) uncertainty is not represented as this is < 1 yr for nearly all samples (smaller than symbol size, reported in Supporting Information Dataset S1).

variation among species (Fig. 3a). Variation in carbon reserve ages was greatest in deep sapwood, and essentially indistinguishable between species in shallow sapwood (Fig. 3a). For example, in *S. sempervirens* the age of carbon reserves stored in 50- to 60-yr-old rings varied by > 25 yr, from < 10 to > 30 yr. Phloem carbon reserve age is less commonly estimated, but ^{14}C mean ages (mean ± SD) were 2.3 ± 2.1 yr (*P. ponderosa*, $n = 2$), *c.* 0 yr (*P. menziesii*, $n = 1$), 6.6 ± 4.8 yr (*S. sempervirens*, $n = 22$), and 3.8 ± 1.7 yr (*P. tremuloides*, $n = 9$).

Nonlinear increases in reserve age with sapwood depth were suggested by the hierarchical statistical model fits for *S. sempervirens*, *P. edulis*, *P. strobus*, and *Q. rubra*, which included quadratic effects for ring number (Bayesian $P < 0.05$, $R^2 \geq 0.8$). The models for *P. strobus*, *Q. rubra*, and *Q. gambelii* were comparatively under determined (one tree per species). The fit for *P. tremuloides* did not include a quadratic term for ring number, as different sites' quadratic effects had opposite signs (Peltier *et al.*, 2023b). Prebomb (60+-yr-old) carbon reserves were present in two conifer species with deep sapwood (*S. sempervirens* and *P. ponderosa*) marked by 'peaked' ^{14}C mean ages at intermediate sapwood depths (Fig. 3b) and negative quadratic effects (Fig. 3a). The highest single observation of $\Delta^{14}C$ was in a beetle-attacked *P. ponderosa*, where $\Delta^{14}C = 180 \pm 1.8‰$ in a subsample containing rings formed in 1954–1974, near the peak of the bomb spike (Fig. 3b). This corresponds to ^{14}C mean age of 36 yr; deeper rings had reduced ^{14}C mean ages reflecting incorporation of atmospheric carbon from before the peak of atmospheric ^{14}C in 1963, implying the ages of these carbon reserves exceed 60+ yr.

Sapwood depth (number of rings) constrains reserve ages

Trees with many (50+) sapwood rings had the oldest maximum ^{14}C mean ages. Maximum ^{14}C mean age was not explained by tree height (Fig. 4a) or DBH (Fig. 4b), but was significantly higher in trees with more sapwood rings ($P < 0.001$, $R^2 = 0.51$; Fig. 4c). For example, trees with DBH that differed by an order of magnitude (e.g. 45 cm vs 450 cm) could have the same maximum ^{14}C mean ages (Fig. 4b). While we lack most tree ages, age does not appear particularly related to maximum ^{14}C mean ages, except as a limitation to sapwood depth for very young trees. For example, the *P. strobus* and *Q. rubra* trees were both *c.* 30 yr old, so could not contain reserves older than 30 yr. Many *S. sempervirens* were 500+ yr old, including the healthy tree in (Fig. 3b), estimated to be 646 yr old (Sillett *et al.*, 2022). Despite such age, the ^{14}C mean age for that individual *S. sempervirens* was

New Phytologist

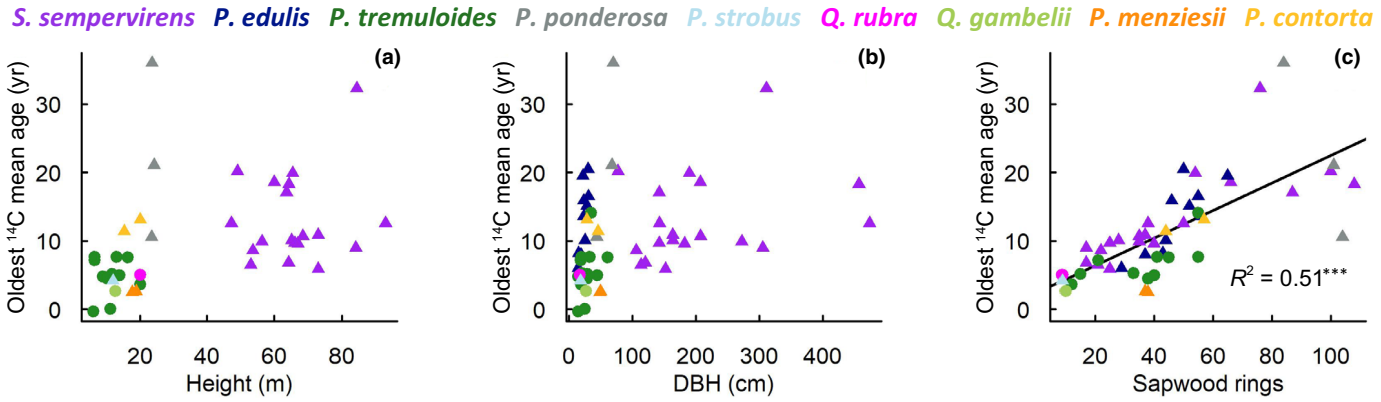

Fig. 4 Maximum carbon reserve ages were related to sapwood depth. The oldest ^{14}C mean ages in each tree were not strongly explained by (a) height of (b) diameter at breast height (DBH). (c) Sapwood ring number explained half the variation across trees in reserve ages (*** indicates $P < 0.001$, $R^2 = 0.51$, linear regression). Tree age is not available for most trees (see the Materials and Methods section).

not exceptional (12.6 ± 0.5 yr), being similar to that of much younger trees of *P. edulis*, *P. ponderosa*, and *P. tremuloides* (Fig. 3a), perhaps due to relatively shallow sapwood (38 rings) of that old *S. sempervirens* individual.

Rapid turnover and deep mixing at steady state

Consistent with rapid respiration of most photosynthate, average turnover time (T) was 2.7 ± 3.5 yr (Fig. 5a, filled symbols), reflecting somewhat longer turnover times of the slow pool ($T_{slow} = 11.0 \pm 9.0$ yr; Fig. 5a, open symbols). Turnover time ranged from 0.5 ± 0.2 yr in *Q. rubra* to 3.7 ± 0.1 yr for *P. edulis*, excepting *P. ponderosa* with distinctly longer $T = 11.5 \pm 0.6$ yr. Average mixing depth of new carbon reserves was 30.2 ± 21.7 rings (Fig. 5b). Mixing depth varied from 5.0 ± 1.6 rings in *Q. rubra* to 56.6 ± 1.8 rings in *P. ponderosa*, where species with mixing depths < 10 rings had shallow sapwood (*Quercus* spp.) or were represented by young trees (e.g. *P. strobus*).

Predictions from the process model (Fig. 6a; $R^2 = 0.85$) followed patterns expected from our theory (Fig. 1; Richardson *et al.*, 2015). For example, *S. sempervirens* and *P. menziesii* had identical $T = 1.3$ yr, but deeper mixing in *P. menziesii* (35 ± 8 vs 26 ± 1 rings) produced younger ^{14}C mean ages in deeper rings (Fig. 6b, purple and orange). Similarly, for two species with similar mixing depths (*P. edulis* vs *P. tremuloides*), longer estimated turnover times produced older ^{14}C mean ages in *P. edulis* falling closer to ring age (closer to 1 : 1 line; Fig. 6b, blue and green).

Stress and disturbance perturb stem reserves

Turnover times and mixing depths estimated in trees not in the steady state are inaccurate, but fitting the model to disturbed trees can test whether disturbances perturb carbon reserve cycling. Accordingly, we estimated a large increase in turnover time for fire ($+15 \pm 0.85$ yr longer than healthy *S. sempervirens*) and bark beetle attack ($+36 \pm 11.5$ yr longer than unattacked *P. ponderosa*). We note however that the results for beetle attack are only based on a single tree. We estimated smaller decreases for experimental drought in *P. edulis* (control: 5.0 ± 0.2 yr vs long-term drought: 2.0 ± 0.2 yr) and natural aridity in *P. tremuloides* (wet site: 11.1 ± 2.4 yr, dry site: 0.4 ± 0.1 yr). Changes in mixing depths were less consistent; deeper in dry site *P. tremuloides* (54.1 ± 0.2 rings) than at a wet site (25.7 ± 3.5 rings), but shorter in *P. edulis* under long-term drought (39.0 ± 4.5 rings) compared with a control (53.1 ± 0.9 rings). These changes corresponded with increases in the relative size of the slow pool for fire (from 25% to 42%) and beetles (from 46% to 93%), and reductions in slow pool size for drought (from 25% to 42%) and aridity (from 53% to 3%). Strikingly, reserves were older than ring age (above the 1 : 1 line) in three burned *S. sempervirens* (Fig. 3b) consistent with 'mixing out' of older reserves from deeper rings.

Discussion

Using a collection of published and newly collected data, we find carbon reserves persist for decades in diverse tree species, longer in the conifer species *S. sempervirens* and *P. ponderosa*. Consistent with theory and previous evidence, the majority of bole reserves is 'young', recent photosynthate soon to be lost to metabolism (Dietze *et al.*, 2014; Richardson *et al.*, 2015; Hartmann & Trumbore, 2016; Sierra *et al.*, 2017). Our synthesis shows new photosynthate is mixed into deep sapwood, so reserves are younger than ring age (Fig. 1; Richardson *et al.*, 2015). For most species, this represents much or all of the sapwood. While turnover time of carbon reserves is generally short, large amounts of decades-old carbon reserves can persist, up to and exceeding 60 yr old in some individual trees, revealed by disturbance (Fig. 3b). Sapwood depth, unlike height or DBH, seems to be the primary constraint on maximum reserve ages, where trees with 60–100+ sapwood rings may contain prebomb carbon reserves (Fig. 4). Very young trees or certain species (perhaps some oaks) then cannot contain old carbon reserves. Our process model captures these dynamics (Fig. 6) and provides a useful framework for simulating carbon reserves in diverse ecological contexts. We highlight the critical role of reserves in tree response to stress and catastrophic

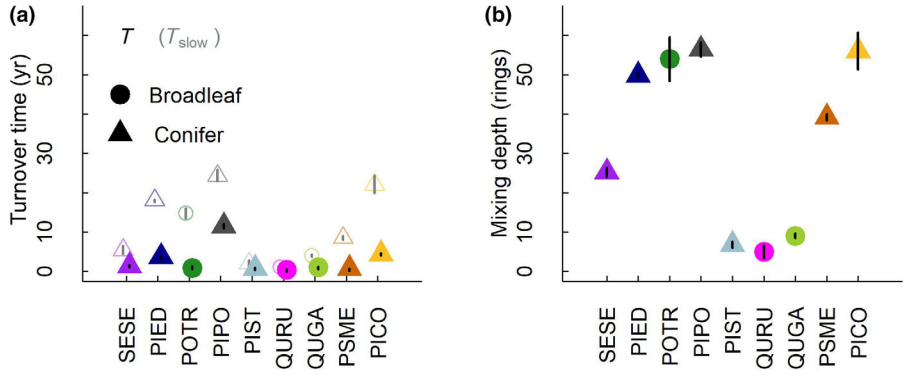

Fig. 5 Parameter estimates from genetic algorithms of (a) turnover time and (b) mixing depth for healthy trees of each species. Vertical lines denote ±1 SD from $n - 1$ leave-one-out parameter estimations (jacknife). In (a), unfilled symbols denote turnover estimates and vertical gray lines denote associated uncertainties (±1 SD) for the slow pool (T_{slow}), from which turnover of the total reserve pool (T) is calculated (see the Materials and Methods section). Species abbreviations are as follows: PICO, *Pinus contorta*; PIED, *Pinus edulis*; PIPO, *Pinus ponderosa*; PIST, *Pinus strobus*; POTR, *Populus tremuloides*; PSME, *Pseudotsuga menziesii*; QUGA, *Quercus gambelii*; QURU, *Quercus rubra*; SESE, *Sequoia sempervirens*.

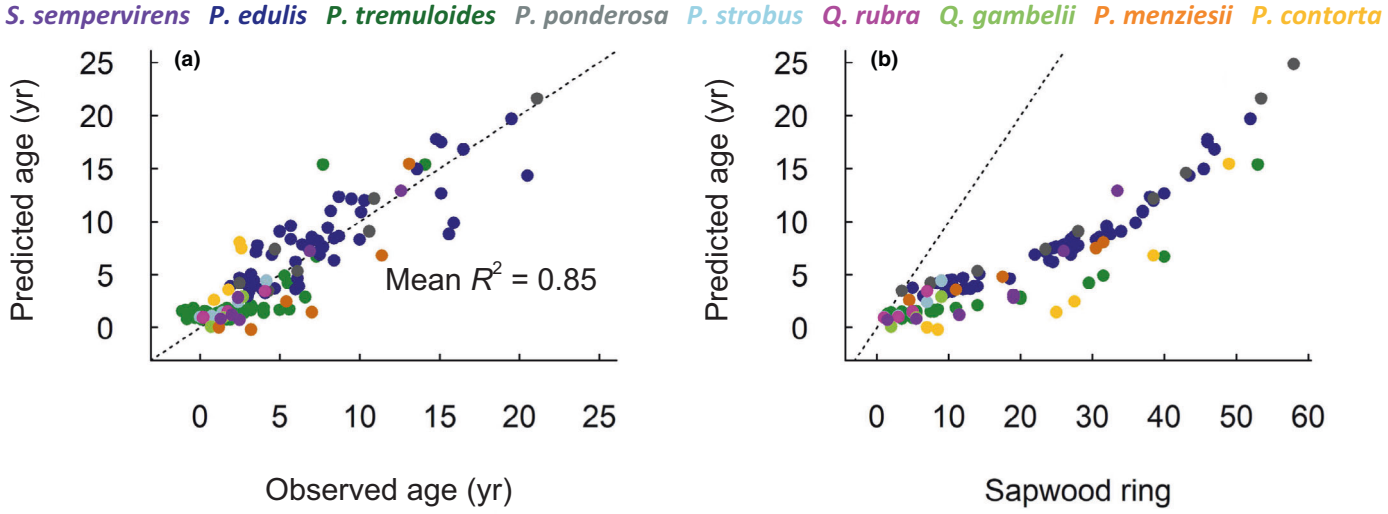

Fig. 6 Predictions of carbon reserve age using selected parameter values from the process-based mixing model plotted against (a) observed ^{14}C mean ages derived from accelerator mass spectrometry (AMS) and (b) sapwood ring ages, with the 1 : 1 line denoted by the diagonal black line. Burned *Sequoia sempervirens* and beetle-attacked *Pinus ponderosa* are omitted, as are prebomb *P. ponderosa* samples (see the Materials and Methods section). In (a), black line denotes a linear regression fit between predicted and observed ages. Reported R^2 is the mean R^2 between predicted and observed across nine species-level regressions (range 0.62–0.99).

disturbance, including direct observations of 'mixing out' (outward translocation of old reserves), in fire-recovering *S. sempervirens*.

Multiple measurements of $\Delta^{14}C$ across sapwood allow interrogation of the heterogeneous mixture of reserves, permitting inference unavailable from single-bole measurements. Or, mean values are a poor way to summarize exponential distributions (Sierra *et al.*, 2017; Herrera-Ramírez *et al.*, 2020), but subsampling can help. To illustrate, we highlight one individual *S. sempervirens* showing the 'peaked' pattern where $\Delta^{14}C$ increases, then decreases with sapwood depth (Fig. 3b). Assuming the deepest samples were fixed before the bomb spike, their measured $\Delta^{14}C$ matches atmospheric $\Delta^{14}C$ in 1957 and 1958. As the deepest subsampled rings roughly span the period of the first *c.* 100 recorded atmospheric nuclear detonations (1946–1955), such measurements represent a mixture of older and younger reserves. Inferring prebomb reserves is impossible with 1 or 2 subsamples; the key evidence is observation of the 'peak' at intermediate sapwood depths (Fig. 3b). For example, one subsample in another tree spans 1913–1949 ($\Delta^{14}C = 57.1‰$), but as we only measured two subsamples, this could imply a ^{14}C mean age of either 15 or 65 yr. To understand the distribution of ages across sapwood tree rings (and thus within a tree's stem reserve pool), subsampling the sapwood by depths (preferably > 3) is essential.

As the major constraint on maximum reserve ages appears to be sapwood longevity, decades-old reserves are probably widespread. Conifers in our dataset contained more sapwood rings

and thus older reserves (Fig. 3b) than angiosperms (Fig. 3c). There are a number of angiosperms that may have deep sapwood, particularly hardwoods in the eastern United States (Carbone *et al.*, 2013), or tropical species (Muhr *et al.*, 2018) with sapwood depths up to 25 cm likely including many years of radial growth (James *et al.*, 2002). Ring-porous *Quercus* spp. may be unlikely to contain very old reserves as they appear to have shallow sapwood (e.g. 7–10 rings here; Fig. 3c) despite abundant ray parenchyma (Williams, 1942) that might serve as mixing 'highways' into heartwood (Fig. 1d; Spicer, 2005). Angiosperms contain larger reserve pools in stems than conifers, due to more abundant axial and ray parenchyma (Lev-Yadun & Aloni, 1995; Godfrey *et al.*, 2020). At the same time, these reserves may turnover more rapidly if they are seasonally drawn down and refilled such as in deciduous trees (Hoch *et al.*, 2003; Furze *et al.*, 2019b). Notably, some *P. tremuloides* here contained 55 sapwood rings, roughly the same depth at which the 'peak' appears in two trees of other species (Fig. 3c). *Populus tremuloides* with slightly deeper sapwood might then contain prebomb reserves. Unfortunately, we only collected single samples of very deep sapwood for this species, as the original study was focused on patterns in shallow sapwood (Peltier *et al.*, 2023d). A broader sampling of species with numerous sapwood rings will likely uncover more species that store old, metabolically available reserves.

Parameter estimates from the process model suggest that reserve ages reflect varied allocation histories of individual trees. Estimates in *P. edulis* under long-term drought and *P. tremuloides* experiencing natural aridity both suggest that trees gradually consume old reserves under prolonged moisture stress, consistent with carbon starvation (McDowell *et al.*, 2022). The model represents this as faster turnover (3–10 yr shorter) and a 40–90% smaller slow pool, such that in both species trees experiencing sustained moisture stress had *c.* 50% younger carbon reserves (Peltier *et al.*, 2023b,d). Changes in mixing depths were not consistent, perhaps because moisture stress may have directly constrained reserve mixing under extreme experimental drought in *P. edulis*, similar to ideas expressed by Sala *et al.* (2010), perhaps via turgor limitation (Sevanto, 2018). By contrast, estimates from trees after abrupt disturbance (wildfire, lethal bark beetle attack) are consistent with major remobilization of the reserve pool, with increases in turnover time of those limited reserves that remain. While consistent with the massive and prolonged resprouting observed in *S. sempervirens* after fire (Peltier *et al.*, 2023a), given we only sampled a single beetle-attacked *P. ponderosa*, additional observations are required to confirm this interpretation for bark beetle infestation. While the process model represents these changes as 15–35 yr increases in turnover time and reduced size of the fast pool, we caution these trees do not meet the steady-state assumptions of our model (Sierra *et al.*, 2017). However, applying the model to disturbed trees has provided evidence consistent with prior work. In past research, girdled trees respired their youngest reserves first, eventually respiring much older reserves after about a year (Muhr *et al.*, 2018). This 'reverse chronological mobilization' could explain very old reserves remaining in these dying or recovering trees, giving the highest ^{14}C mean ages in our dataset ($\Delta^{14}C = 157 \pm 2.6‰$ in *S. sempervirens*, $\Delta^{14}C = 180 \pm 1.8‰$ in *P. ponderosa*). But additional model development to explicitly account for changes to steady state is required to validate such interpretations.

Alternatively, very high ^{14}C mean ages in disturbed trees could reflect redistribution of old reserves to shallower sapwood under lethal stress. Three burned *S. sempervirens* had carbon reserve ages in shallow rings exceeding ring age (above the 1 : 1 line; Fig. 3b). For one *S. sempervirens*, the shallowest subsample includes the most recently formed nine rings, but the ^{14}C mean age of reserves in this sample was 18 ± 0.6 yr (Fig. 3b). To our knowledge, this is the first direct observation of reserves being 'mixed out' (Fig. 1a), that is, old reserves in transit across the sapwood. However, this should not be surprising given previous direct evidence of old reserve remobilization to build new roots (Vargas *et al.*, 2009) or leaves (Carbone *et al.*, 2013; D'Andrea *et al.*, 2019) after disturbance, up to many decades old in some cases (Peltier *et al.*, 2023a). The frequency and magnitude of translocation of old reserves (as opposed to the movement of new photosynthate) are essentially unknown, but may be most likely under catastrophic disturbance. However, whether or not more limited 'mixing out' occurs more frequently under less extreme conditions is essentially unknown. Our process model may provide a way to test expectations against observations to investigate the prevalence of old reserve mobilization in broad ecological contexts. For example, the model appears to be a useful way to distinguish trees whose carbon reserve pools are or are not at the steady state.

Conclusions

Past work has shown that substantial variability in annual productivity can be explained by previous-year carbon uptake (Gough *et al.*, 2009; Teets *et al.*, 2022), previous-year climate conditions (Peltier *et al.*, 2018), or past perturbation of carbon uptake (Anderegg *et al.*, 2015), suggesting that stored reserves, even old reserves, play a major role in ongoing metabolism (Körner, 2003; Carbone & Trumbore, 2007; Muhr *et al.*, 2013; Dietze *et al.*, 2014; Trumbore *et al.*, 2015; Peltier *et al.*, 2023b). Sapwood is typically the largest pool of reserves (Hoch *et al.*, 2003) and simple calculations with our data suggest that the global mass of sapwood reserves in temperate forests could be as large as 0.1 petagrams (Thurner *et al.*, 2019). While our dataset is not representative of global sapwood (we sampled no seedlings or saplings), the mean mass-weighted average age of whole-tree carbon reserves is 4.25 yr. Yet, consideration of labile carbon in vegetation models beyond a single pool is to our knowledge nonexistent, and sapwood carbon reserves remain among the most poorly understood reservoirs of carbon reserves in trees. Maximum ages of carbon reserves appear primarily constrained by sapwood depth (number of sapwood rings), suggesting that prebomb reserves are unlikely to be unique to conifers. Investigating the spatial distribution and persistence of old carbon reserves can improve our understanding of both carbon allocation and the cycling of labile photosynthate in forest ecosystems. Widespread old reserves imply that, at the very least, improved representation of carbon allocation in vegetation models (e.g. Worden *et al.*, 2024) should be a priority.

Acknowledgements

DMPP acknowledges support from NSF-IOS-RAPID grants no. 1936205 and no. 2053337, NSF-DEB award no. 2213599, and grant no. 149 from the Save the Redwoods League. ADR acknowledges support from NSF-DEB award #1832218. We acknowledge Tim Rademacher for the inspiration of Fig. 1(d). We thank an anonymous reviewer for helpful suggestions for improving the process model.

Competing interests

None declared.

Author contributions

DMPP collected and assembled data with advice from ADR, MSC, KO and GK. ADR and DMPP developed the mixing process model. DMPP implemented the modeling analyses and drafted the manuscript and figures. All authors contributed to revisions.

ORCID

Mariah S. Carbone https://orcid.org/0000-0002-7832-7009
George W. Koch https://orcid.org/0000-0001-6020-9250
Kiona Ogle https://orcid.org/0000-0002-0652-8397
Drew M. P. Peltier https://orcid.org/0000-0003-3271-9055
Andrew D. Richardson https://orcid.org/0000-0002-0148-6714

Data availability

Full dataset and process model, along with a readme file, and a script demonstrating parameter estimation routine, are directly available in the Supporting Information (Dataset S1; Methods S1, S2).

References

Adams HD, Germino MJ, Breshears DD, Barron-Gafford GA, Guardiola-Claramonte M, Zou CB, Huxman TE. 2013. Nonstructural leaf carbohydrate dynamics of *Pinus edulis* during drought-induced tree mortality reveal role for carbon metabolism in mortality mechanism. *New Phytologist* **197**: 1142–1151.

Anderegg WRL, Anderegg LD. 2013. Hydraulic and carbohydrate changes in experimental drought-induced mortality of saplings in two conifer species. *Tree Physiology* **33**: 252–260.

Anderegg WRL, Callaway ES. 2012. Infestation and hydraulic consequences of induced carbon starvation. *Plant Physiology* **159**: 1866–1874.

Anderegg WRL, Schwalm C, Biondi F, Camarero JJ, Koch G, Litvak M, Ogle K, Shaw JD, Shevliakova E, Williams AP *et al.* 2015. Pervasive drought legacies in forest ecosystems and their implications for carbon cycle models. *Science* **349**: 528–532.

Barbaroux C, Bréda N. 2002. Contrasting distribution and seasonal dynamics of carbohydrate reserves in stem wood of adult ring-porous sessile oak and diffuse-porous beech trees. *Tree Physiology* **22**: 1201–1210.

Blumstein M, Oseguera M, Caso-McHugh T, Des Marais DL. 2024. Nonstructural carbohydrate dynamics' relationship to leaf development under varying environments. *New Phytologist* **241**: 102–113.

Carbone MS, Czimczik CI, Keenan TF, Murakami PF, Pederson N, Schaberg PG, Xu X, Richardson AD. 2013. Age, allocation and availability of nonstructural carbon in mature red maple trees. *New Phytologist* **200**: 1145–1155.

Carbone MS, Trumbore SE. 2007. Contribution of new photosynthetic assimilates to respiration by perennial grasses and shrubs: residence times and allocation patterns. *New Phytologist* **176**: 124–135.

Chapin FS III, Schulze ED, Mooney HA. 1990. The ecology and economics of storage in plants. *Annual Review of Ecology and Systematics* **21**: 423–447.

Chow PS, Landhäusser SM. 2004. A method for routine measurements of total sugar and starch content in woody plant tissues. *Tree Physiology* **24**: 1129–1136.

Czimczik CI, Trumbore SE, Xu XM, Carbone MS. 2014. Extraction of nonstructural carbon and cellulose from wood for radiocarbon analysis. *Bio-Protocol* **4**: e1169.

D'Andrea E, Rezaie N, Battistelli A, Gavrichkova O, Kuhlmann I, Matteucci G, Moscatello S, Proietti S, Scartazza A, Trumbore S. 2019. Winter's bite: beech trees survive complete defoliation due to spring late-frost damage by mobilizing old C reserves. *New Phytologist* **224**: 625–631.

Dickman LT, McDowell NG, Sevanto S, Pangle RE, Pockman WT. 2015. Carbohydrate dynamics and mortality in a piñon-juniper woodland under three future precipitation scenarios. *Plant, Cell & Environment* **38**: 729–739.

Dietze MC, Sala A, Carbone MS, Czimczik CI, Mantooth JA, Richardson AD, Vargas R. 2014. Nonstructural carbon in woody plants. *Annual Review of Plant Biology* **65**: 667–687.

Epron D, Bahn M, Derrien D, Lattanzi FA, Pumpanen J, Gessler A, Högberg P, Maillard P, Dannoura M, Gérant D *et al.* 2012. Pulse-labelling trees to study carbon allocation dynamics: a review of methods, current knowledge and future prospects. *Tree Physiology* **32**: 776–798.

Furze ME, Drake JE, Wiesenbauer J, Richter A, Pendall E. 2019a. Carbon isotopic tracing of sugars throughout whole-trees exposed to climate warming. *Plant, Cell & Environment* **42**: 3253–3263.

Furze ME, Huggett BA, Aubrecht DM, Stolz CD, Carbone MS, Richardson AD. 2019b. Whole-tree nonstructural carbohydrate storage and seasonal dynamics in five temperate species. *New Phytologist* **221**: 1466–1477.

Furze ME, Huggett BA, Chamberlain CJ, Wieringa MM, Aubrecht DM, Carbone MS, Walker JC, Xu X, Czimczik CI, Richardson AD. 2020. Seasonal fluctuation of nonstructural carbohydrates reveals the metabolic availability of stemwood reserves in temperate trees with contrasting wood anatomy. *Tree Physiology* **40**: 1355–1365.

Godfrey JM, Riggio J, Orozco J, Guzmán-Delgado P, Chin AR, Zwieniecki MA. 2020. Ray fractions and carbohydrate dynamics of tree species along a 2750 m elevation gradient indicate climate response, not spatial storage limitation. *New Phytologist* **225**: 2314–2330.

Gough CM, Flower CE, Vogel CS, Dragoni D, Curtis PS. 2009. Whole-ecosystem labile carbon production in a north temperate deciduous forest. *Agricultural and Forest Meteorology* **149**: 1531–1540.

Hagedorn F, Joseph J, Peter M, Luster J, Pritsch K, Geppert U, Kerner R, Molinier V, Egli S, Schaub M *et al.* 2016. Recovery of trees from drought depends on belowground sink control. *Nature Plants* **2**: 16111.

Hartmann H, Trumbore S. 2016. Understanding the roles of nonstructural carbohydrates in forest trees – from what we can measure to what we want to know. *New Phytologist* **211**: 386–403.

Herrera-Ramírez D, Muhr J, Hartmann H, Römermann C, Trumbore S, Sierra CA. 2020. Probability distributions of nonstructural carbon ages and transit times provide insights into carbon allocation dynamics of mature trees. *New Phytologist* **226**: 1299–1311.

Hesse BD, Hartmann H, Rötzer T, Landhäusser SM, Goisser M, Weikl F, Pritsch K, Grams TE. 2021. Mature beech and spruce trees under drought – higher C investment in reproduction at the expense of whole-tree NSC stores. *Environmental and Experimental Botany* **191**: 104615.

Hoch G, Richter A, Körner C. 2003. Non-structural carbon compounds in temperate forest trees. *Plant, Cell & Environment* **26**: 1067–1081.

Hua Q, Turnbull JC, Santos GM, Rakowski AZ, Ancapichún S, De Pol-Holz R, Hammer S, Lehman SJ, Levin I, Miller JB. 2022. Atmospheric radiocarbon for the period 1950–2019. *Radiocarbon* **64**: 723–745.

Huang J, Hammerbacher A, Gershenzon J, van Dam NM, Sala A, McDowell NG, Chowdhury S, Gleixner G, Trumbore S, Hartmann H. 2021. Storage of carbon

reserves in spruce trees is prioritized over growth in the face of carbon limitation. *Proceedings of the National Academy of Sciences, USA* **118**: e2023297118.

Huang J, Hammerbacher A, Weinhold A, Reichelt M, Gleixner G, Behrendt T, Van Dam NM, Sala A, Gershenzon J, Trumbore S. 2019. Eyes on the future–evidence for trade-offs between growth, storage and defense in Norway spruce. *New Phytologist* **222**: 144–158.

Ichie T, Igarashi S, Yoshida S, Kenzo T, Masaki T, Tayasu I. 2013. Are stored carbohydrates necessary for seed production in temperate deciduous trees? *Journal of Ecology* **101**: 525–531.

James SA, Clearwater MJ, Meinzer FC, Goldstein G. 2002. Heat dissipation sensors of variable length for the measurement of sap flow in trees with deep sapwood. *Tree Physiology* **22**: 277–283.

Kabeya D, Iio A, Kakubari Y, Han Q. 2021. Dynamics of non-structural carbohydrates following a full masting event reveal a role for stored starch in relation to reproduction in *Fagus crenata*. *Forest Research* **1**: 1–10.

Kagawa A, Sugimoto A, Maximov TC. 2006. Seasonal course of translocation, storage and remobilization of ^{13}C pulse-labeled photoassimilate in naturally growing *Larix gmelinii* saplings. *New Phytologist* **171**: 793–804.

Kobe RK. 1997. Carbohydrate allocation to storage as a basis of interspecific variation in sapling survivorship and growth. *Oikos* **80**: 226–233.

Körner C. 2003. Carbon limitation in trees. *Journal of Ecology* **91**: 4–17.

Levin I, Kromer B. 2004. The tropospheric $^{14}CO_2$ level in mid latitudes of the northern hemisphere (1959–2003). *Radiocarbon* **46**: 1261–1271.

Lev-Yadun S, Aloni R. 1995. Differentiation of the ray system in woody plants. *The Botanical Review* **61**: 45–84.

Lowe DC. 1984. Preparation of graphite targets for radiocarbon dating by tandem accelerator mass spectrometer (TAMS). *The International Journal of Applied Radiation and Isotopes* **35**: 349–352.

McDowell NG, Sapes G, Pivovaroff A, Adams HD, Allen CD, Anderegg WRL, Arend M, Breshears DD, Brodribb T, Choat B *et al.* 2022. Mechanisms of woody plant mortality under rising drought, CO_2, and vapor pressure deficit. *Nature Reviews Earth and Environment* **3**: 294–308.

Metzler H, Müller M, Sierra CA. 2018. Transit-time and age distributions for nonlinear time-dependent compartmental systems. *Proceedings of the National Academy of Sciences* **115**: 1150–1155.

Morris H, Plavcová L, Cvecko P, Fichtler E, Gillingham MA, Martínez-Cabrera HI, McGlinn DJ, Wheeler E, Zheng J, Ziemińska K *et al.* 2015. A global analysis of parenchyma tissue fractions in secondary xylem of seed plants. *New Phytologist* **209**: 1553–1565.

Muhr J, Angert A, Negrón-Juárez RI, Muñoz WA, Kraemer G, Chambers JQ, Trumbore SE. 2013. Carbon dioxide emitted from live stems of tropical trees is several years old. *Tree Physiology* **33**: 743–752.

Muhr J, Messier C, Delagrange S, Trumbore S, Xu X, Hartmann H. 2016. How fresh is maple syrup? Sugar maple trees mobilize carbon stored several years previously during early springtime sap-ascent. *New Phytologist* **209**: 1410–1416.

Muhr J, Trumbore S, Higuchi N, Kunert N. 2018. Living on borrowed time – Amazonian trees use decade-old storage carbon to survive for months after complete stem girdling. *New Phytologist* **220**: 111–120.

Nakaba S, Kubo T, Funada R. 2008. Differences in patterns of cell death between ray parenchyma cells and ray tracheids in the conifers *Pinus densiflora* and *Pinus rigida*. *Trees* **22**: 623–630.

Oswald SW, Aubrey DP. 2023. Modeling starch dynamics from seasonal variations of photosynthesis, growth and respiration. *Tree Physiology* tpad007.

Palacio S, Hoch G, Sala A, Körner C, Millard P. 2014. Does carbon storage limit tree growth? *New Phytologist* **201**: 1096–1100.

Peltier DMP, Barber JJ, Ogle K. 2018. Quantifying antecedent climatic drivers of tree growth in the Southwestern US. *Journal of Ecology* **106**: 613–624.

Peltier DMP, Carbone MS, Enright M, Marshall MC, Trowbridge AM, LeMoine JM, Koch GW, Richardson AD. 2023a. Old reserves and ancient buds fuel regrowth of coast redwood after catastrophic fire. *Nature Plants* **9**: 1978–1985.

Peltier DMP, Carbone MS, McIntire CD, Robertson N, Thompson RA, Malone S, LeMoine J, Richardson AD, McDowell NG, Adams HD. 2023b. Carbon starvation following a decade of experimental drought consumes old reserves in *Pinus edulis*. *New Phytologist* **240**: 92–104.

Peltier DMP, LeMoine J, Ebert C, Xu X, Ogle K, Richardson A, Carbone M. 2023c. An incubation method to determine the age of available nonstructural carbon in woody plant tissues. *Tree Physiology* tpad015.

Peltier DMP, Nguyen P, Ebert C, Koch GW, Schuur EA, Ogle K. 2023d. Moisture stress limits radial mixing of non-structural carbohydrates in sapwood of trembling aspen. *Tree Physiology* tpad083.

Piovesan G, Biondi F. 2021. On tree longevity. *New Phytologist* **231**: 1318–1337.

Plummer M. 2003. JAGS: a program for analysis of Bayesian graphical models using Gibbs sampling. In: *Proceedings of the 3rd international workshop on distributed statistical computing*. Vienna, Austria, 125. [WWW document] URL https://www.r-project.org/conferences/DSC-2003/Proceedings/Plummer.pdf [accessed 28 November 2024].

Plummer M. 2013. *rjags: Bayesian graphical models using MCMC*. R package v.3–10. [WWW document] URL https://cran.r-project.org/web/packages/rjags/ [accessed 22 November 2024].

R Core Team. 2022. *R: a language and environment for statistical computing*. Vienna, Austria: R Foundation for Statistical Computing.

Reed CC, Hood SM. 2023. Nonstructural carbohydrates explain post-fire tree mortality and recovery patterns. *Tree Physiology* tpad155.

Rehschuh R, Rehschuh S, Gast A, Jakab A, Lehmann MM, Saurer M, Gessler A, Ruehr NK. 2022. Tree allocation dynamics beyond heat and hot drought stress reveal changes in carbon storage, belowground translocation and growth. *New Phytologist* **233**: 687–704.

Reimer PJ, Brown TA, Reimer RW. 2004. Discussion: reporting and calibration of post-bomb ^{14}C data. *Radiocarbon* **46**: 1299–1304.

Richardson AD, Carbone MS, Huggett BA, Furze ME, Czimczik CI, Walker JC, Xu X, Schaberg PG, Murakami P. 2015. Distribution and mixing of old and new nonstructural carbon in two temperate trees. *New Phytologist* **206**: 590–597.

Sala A, Piper F, Hoch G. 2010. Physiological mechanisms of drought-induced tree mortality are far from being resolved. *New Phytologist* **186**: 274–281.

Sala A, Woodruff DR, Meinzer FC. 2012. Carbon dynamics in trees: feast or famine? *Tree Physiology* **32**: 764–775.

Schädel C, Blöchl A, Richter A, Hoch G. 2009. Short-term dynamics of nonstructural carbohydrates and hemicelluloses in young branches of temperate forest trees during bud break. *Tree Physiology* **29**: 901–911.

Sevanto S. 2018. Drought impacts on phloem transport. *Current Opinion in Plant Biology* **43**: 76–81.

Sierra CA, Müller M, Metzler H, Manzoni S, Trumbore SE. 2017. The muddle of ages, turnover, transit, and residence times in the carbon cycle. *Global Change Biology* **23**: 1763–1773.

Sillett SC, Antoine ME, Carroll AL, Graham ME, Chin AR, Van Pelt R. 2022. Rangewide climatic sensitivities and non-timber values of tall *Sequoia sempervirens* forests. *Forest Ecology and Management* **526**: 120573.

Spicer R. 2005. Senescence in secondary xylem: heartwood formation as an active developmental program. In: Holbrook NM, Zwieniecki MA, eds. *Vascular transport in plants*. Academic Press, 457–475.

Spicer R, Holbrook NM. 2007. Parenchyma cell respiration and survival in secondary xylem: does metabolic activity decline with cell age? *Plant, Cell & Environment* **30**: 934–943.

Stuiver M, Polach HA. 1977. Discussion reporting of ^{14}C data. *Radiocarbon* **19**: 355–363.

Synal H-A, Stocker M, Suter M. 2007. MICADAS: a new compact radiocarbon AMS system. *Nuclear Instruments and Methods in Physics Research Section B: Beam Interactions with Materials and Atoms* **259**: 7–13.

Teets A, Moore DJP, Alexander MR, Blanken PD, Bohrer G, Burns SP, Carbone MS, Ducey MJ, Fraver S, Gough CM *et al.* 2022. Coupling of tree growth and photosynthetic carbon uptake across six north American forests. *Journal of Geophysical Research: Biogeosciences* **127**: e2021JG006690.

Thurner M, Beer C, Crowther T, Falster D, Manzoni S, Prokushkin A, Schulze E. 2019. Sapwood biomass carbon in northern boreal and temperate forests. *Global Ecology and Biogeography* **28**: 640–660.

Trumbore S, Czimczik CI, Sierra CA, Muhr J, Xu X. 2015. Non-structural carbon dynamics and allocation relate to growth rate and leaf habit in California oaks. *Tree Physiology* **35**: 1206–1222.

Trumbore SE, Sierra CA, Pries CH. 2016. Radiocarbon nomenclature, theory, models, and interpretation: measuring age, determining cycling rates, and tracing source pools. In: Schuur E, Druffel E, Trumbore S, eds. *Radiocarbon and climate change*. Cham, Switzerland: Springer, 45–82.

Vargas R, Trumbore SE, Allen MF. 2009. Evidence of old carbon used to grow new fine roots in a tropical forest. *New Phytologist* **182**: 710–718.

Vogel JS, Southon JR, Nelson DE, Brown TA. 1984. Performance of catalytically condensed carbon for use in accelerator mass spectrometry. *Nuclear Instruments and Methods in Physics Research Section B: Beam Interactions with Materials and Atoms* **5**: 289–293.

Wiley E, Rogers BJ, Hodgkinson R, Landhäusser SM. 2016. Nonstructural carbohydrate dynamics of lodgepole pine dying from mountain pine beetle attack. *New Phytologist* **209**: 550–562.

Williams S. 1942. Secondary vascular tissues of the oaks indigenous to the United States-III. A comparative anatomical study of the wood of *Leucobalanus* and *Erythrobalanus*. *Bulletin of the Torrey Botanical Club* **69**: 115–129.

Worden MA, Famiglietti CA, Levine PA, Ma S, Bloom AA, Bonal D, Stahl C, Konings AG. 2024. Inferred drought-induced plant allocation shifts and their impact on drought legacy at a tropical forest site. *Global Change Biology* **30**: e17287.

Supporting Information

Additional Supporting Information may be found online in the Supporting Information section at the end of the article.

Dataset S1 Full AMS dataset and associated trait values and study information.

Methods S1 JAGS model code to infer age vs depth trends.

Methods S2 Process model code and example.

Please note: Wiley is not responsible for the content or functionality of any Supporting Information supplied by the authors. Any queries (other than missing material) should be directed to the *New Phytologist* Central Office.

Disclaimer: The New Phytologist Foundation remains neutral with regard to jurisdictional claims in maps and in any institutional affiliations.